Hall Thruster Plume Measurements On-board the Russian Express Satellites

David Manzella
The University of Toledo
Toledo, OH 43606

Robert Jankovsky & Frederick Elliott
NASA John H. Glenn Research Center
Cleveland, OH 44135

Ioannis Mikellides & Gary Jongeward
Science Applications International Corporation
San Diego, CA 92121

Doug Allen
Schafer Corporation
Dayton, OH 45431

The operation of North-South and East-West station-keeping Hall thruster propulsion systems on-board two Russian Express-A geosynchronous communication satellites were investigated through a collaborative effort with the manufacturer of the spacecraft. Over 435 firings of sixteen different thrusters with a cumulative run time of over 550 hours were reported with no thruster failures. Momentum transfer due to plume impingement was evaluated based on reductions in the effective thrust of the SPT-100 thrusters and induced disturbance torques determined based on attitude control system data and range data. Hall thruster plasma plume effects on the transmission of C-band and Ku-band communication signals were shown to be negligible. On-orbit ion current density measurements were made and subsequently compared to predictions and ground test data. Ion energy, total pressure, and electric field strength measurements were also measured on-orbit. The effect of Hall thruster operation on solar array performance over several months was investigated. A subset of these data is presented.

Introduction

Following the successful acceptance testing and delivery of an experimental one kilowatt Hall thruster system in 1997 the United States Department of Defense's Ballistic Missile Defense Organization (BMDO) embarked on a program to demonstrate a 4.5 kilowatt joint U.S./Russian Hall thruster system on-board a Russian geosynchronous communication satellite.[1] This program, managed by the NASA Glenn Research Center (GRC), was designed to integrate a 4.5 kW T160E Hall thruster and xenon flow control unit provided by the Keldysh Research Center of Moscow, Russia with a power processing unit designed and built by Space Power Incorporated of San Jose, California. Space Power was the prime contractor for the program. During the implementation of this project BMDO redirected its efforts away from a space based defense system. The NASA Future-X Pathfinder Program Office at the Marshall Space Flight Center was enlisted to support the completion of the space flight hardware and its integration on to the spacecraft.[2] Additionally, the scope of the project was increased to include diagnostic measurements on-board the spacecraft with the T160E as well as a second identical Russian geosynchronous communication satellite to be launched prior to the one carrying the 4.5 kW propulsion system. Due to development difficulties and schedule constraints the T160E propulsion system was not integrated on-board the spacecraft following successful completion of a functional ground test. The diagnostic capabilities were however integrated onto both satellites. This paper describes these Russian geosynchronous communication satellites, the Hall thruster propulsion systems they utilize, the on-board diagnostics they employ, and presents a subset of the on-orbit data obtained to date. The entire body of this information can be found in various reports provided under contract to NASA GRC by Space Power (who has since become a part of Pratt & Whitney's Space Propulsion and Chemical Systems Division) and their subcontractors on this program.[3-9]

Spacecraft

The on-orbit diagnostic measurements were made on-board two Russian geosynchronous communication satellites. These two satellites are the second and third in the series of Express-A spacecraft. These spacecraft which are designed for a minimum 7-year lifetime are 2600 kg, 3-axis stabilized, geosynchronous communication satellites with 2.5 kilowatts of power at the beginning of life. The spacecraft bus was designed and constructed by NPO Prikladnoy Mekhaniki (NPO-PM) of Zheleznogorsk, Russia which also provided integration of the payload consisting of 12 C-band and 5 Ku-band transponders provided by Alcatel Espace of France. Both spacecraft were launched aboard Proton launch vehicles from the Baikonur

Cosmodrome in Kazakhstan. Express-A #2, which was launched on March 12, 2000, is currently on station at 80 degrees East and is being used for Russian television broadcasts and dedicated network operation. Express-A #3, which was launched on June 24, 2000, replaced the aging Statsionar-11 (Gorizont-26) at an orbital position of 11 degrees West and is being used for high-speed Internet access to the Middle East and Africa from Europe.

Propulsion System

The on-orbit propulsion system for each spacecraft consists of four orbital control thruster units, the xenon feed unit (XFU), three xenon storage units, and the power-processing unit. Each thruster control unit, provided by Fakel Enterprises of Kaliningrad, Russia, contains two SPT-100 Hall thrusters each with a redundant cathode and the necessary propellant valves, flow restrictors and thermo-throttles. A general view of an orbital control thruster unit is shown in Figure 1. On-board Express-A #2 the three xenon propellant tanks were loaded with 85.5 kg of xenon. Express-A #3 carried 88.3 kg of xenon into orbit.

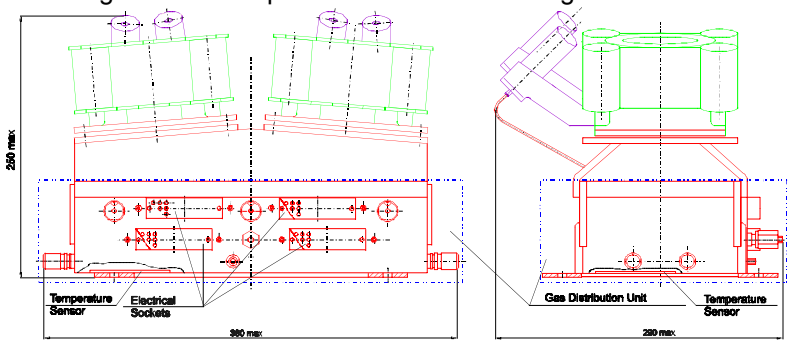

Figure 1: Orbital Control Thruster Unit

With respect to nomenclature each thruster control unit is designated as TU1, TU2, TU3, or TU4. The two thrusters located within each thruster control unit are designated based on whether it is the primary or redundant thruster (T# or RT#) and whether it is the primary or redundant cathode for that thruster (C1 or C2). So, for example, the primary thruster and cathode of TU2 is designated T2C1 and the redundant thruster and cathode for TU3 is RT3C2. TU1 and TU2 are used for east-west station keeping and TU3 and TU4 are used for north-south station keeping. Each thruster within the thruster control unit is positioned with a 5˚ 40’ angle with respect to ideal north-south or east-west direction passing through the spacecraft center of gravity. A schematic of the Express-A spacecraft design is shown in Figure 2.

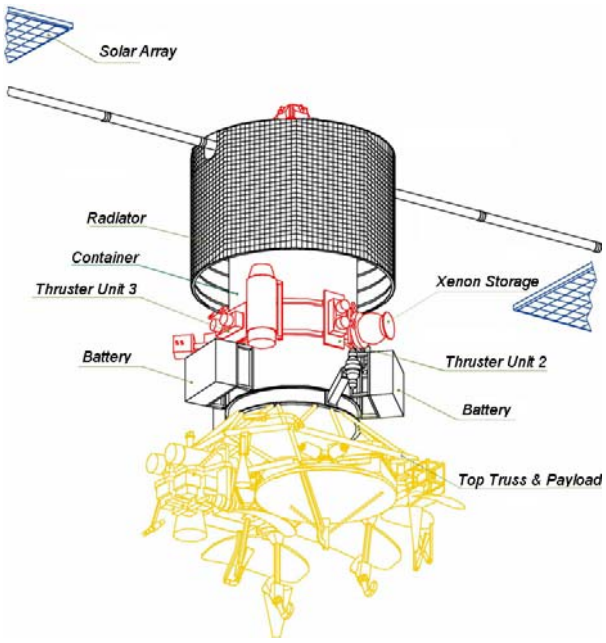

Figure 2: Express-A spacecraft design

The performance of each thruster cathode combination was measured at the nominal 300 Volts discharge voltage and 4.5 Amperes discharge current as part of the acceptance test program. These data are shown in Table 1.

Table 1: SPT-100 Acceptance Test Measured Performance

Satellite	Thruster	Cathode	Thrust
Express-A #2	T1	C1	84.80 mN
Express-A #2	T1	C2	84.60 mN
Express-A #2	RT1	C1	82.80 mN
Express-A #2	RT1	C2	82.40 mN
Express-A #2	T2	C1	86.60 mN
Express-A #2	T2	C2	85.50 mN
Express-A #2	RT2	C1	85.50 mN
Express-A #2	RT2	C2	84.50 mN
Express-A #2	T3	C1	84.00 mN
Express-A #2	T3	C2	83.20 mN
Express-A #2	RT3	C1	83.60 mN
Express-A #2	RT3	C2	83.60 mN
Express-A #2	T4	C1	80.20 mN
Express-A #2	T4	C2	81. 10 mN
Express-A #2	RT4	C1	84.30 mN
Express-A #2	RT4	C2	83.70 mN
Express-A #3	T1	C1	84.28 mN
Express-A #3	T1	C2	83.89 mN
Express-A #3	RT1	C1	85.85 mN
Express-A #3	RT1	C2	85.65 mN
Express-A #3	T2	C1	84.77 mN
Express-A #3	T2	C2	84.48 mN
Express-A #3	RT2	C1	83.50 mN
Express-A #3	RT2	C2	83.50 mN
Express-A #3	T3	C1	83.89 mN
Express-A #3	T3	C2	84.08 mN
Express-A #3	RT3	C1	85.26 mN
Express-A #3	RT3	C2	84.67 mN
Express-A #3	T4	C1	82.81 mN
Express-A #3	T4	C2	82.81 mN
Express-A #3	RT4	C1	85.06 mN
Express-A #3	RT4	C2	84.67 mN

Once on orbit each thruster and cathode configuration were functioned twice for two minutes each to demonstrate serviceability. Following this the SPT-100s were used to position the spacecraft at the desired station point at which time continued use was for normal station keeping maneuvers. On Express-A #2 from March 12, 2000 to June 15, 2000 the following firings were executed.

Table 2: Express-A #2 SPT-100 firing history for March 12, 2000 to June 15, 2000

Thruster	Cathode	Total firing duration, hh:mm:ss	Number of firings
T1	C1	20:15:04	3
T1	C2	00:05:50	2
RT1	C1	17:50:50	3
RT1	C2	00:05:50	2
T2	C1	23:15:50	8
T2	C2	00:05:50	2
RT2	C1	36:05:50	3
RT2	C2	00:05:50	2
T3	C1	26:51:38	36
T3	C2	00:05:50	2
RT3	C1	28:00:06	33
RT3	C2	00:05:50	2
T4	C1	19:42:28	26
T4	C2	00:05:50	2
RT4	C1	06:05:50	19
RT4	C2	00:05:50	2

On Express-A #3 from June 24, 2000 to March 31, 2001 the following firings were executed.

Table 3: Express-A #2 SPT-100 firing history for June 24, 2000 to March 31, 2001

Thruster	Cathode	Total firing duration, hh:mm:ss	Number of firings
T1	C1	02:05:50	4
T1	C2	00:05:50	2
RT1	C1	98:30:50	8
RT1	C2	00:05:50	2
T2	C1	01:05:50	3
T2	C2	00:05:50	2
RT2	C1	03:35:50	5
RT2	C2	00:05:50	2
T3	C1	14:11:46	24
T3	C2	00:05:50	2
RT3	C1	23:06:42	32
RT3	C2	00:05:50	2
T4	C1	80:07:55	67
T4	C2	33:48:58	29
RT4	C1	89:27:80	77
RT4	C2	31:57:22	27

Additional data from operation of the propulsion system on-board Express-A #3 from July 1, 2001 to September 30, 2001 will also be provided. The longest single firing was 48 hours and 20 minutes. Several other long duration firings occurred during the final positioning of each spacecraft. The on-board telemetry obtained from the propulsion system consisted of: thruster selected, cathode selected, anode voltage, anode current, temperature of each of the xenon storage units (propellant tanks), the temperature of the xenon feed units (XFU), and the temperatures of each of the thruster units. Data is taken at a frequency of 0.2 Hz. As an example of the in-flight data the anode voltage and anode current for operation of T4C1 on April 17, 2000 aboard Express-A #2 is shown in Figure 3.

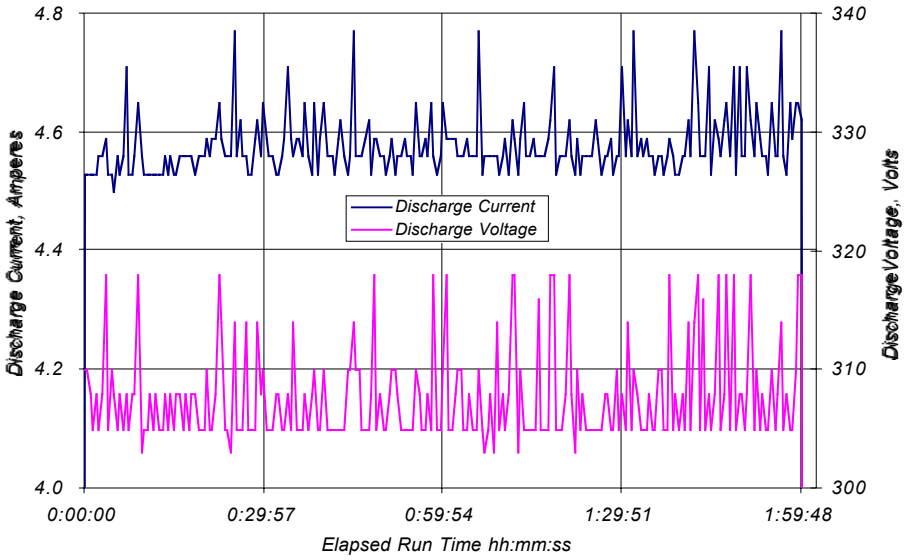

Figure 3: Discharge Voltage and Discharge current versus time for T4C1 firing on 4/17/00

As can be seen there are significant fluctuations with respect to both anode current and anode voltage. Also the average discharge current was 4.6 Amperes and the average discharge voltage was 310 Volts. Differences between the on-orbit measured values of anode voltage and current and the acceptance test values of 4.5 Amperes and 300 Volts were consistent for each thruster and all the firings. The voltage difference is attributed to the power-processing unit (PPU) having an unregulated output and the thrusters being operated when the bus voltage was near the top of its operating range. The current difference is attributed to the flight PPU and thrusters not being functioned together during the ground test program to accurately set the current regulation set point. The total xenon mass flow rate through the thruster and

cathode at this operating point is not known, nor was the xenon mass flow rate from the acceptance tests provided. For other SPT-100s the total mass flow rate specification at 4.5 Amperes of discharge current is 5.3 mg/sec, although this may vary slightly from thruster to thruster. The cathode flow fraction is approximately 7%, so the nominal anode flow rate is 4.9 mg/sec.

On-Board Sensors

Several on-board sensors were integrated onto both Express-A #2 and Express-A #3 in order to get information on how the satellite's environment was altered by operation of the Hall thrusters. On-board Express-A #2 were three electric field strength sensors and two ion current density sensors. The electric field strength sensors (designated DEP), which were designed to measure electric field strength in the range of $\pm 2 \times 10^5$ Volts/meter, operated by sensing changes in the potential of an oscillating ferromagnetic electrode. The change in potential in the electrode as it vibrated was proportional to the field strength. These probes were calibrated in a vacuum chamber in the presence of a static electric field. The uncertainty in electric field measurements was estimated to be not more than 20%. This sensor is shown schematically in Figure 4.

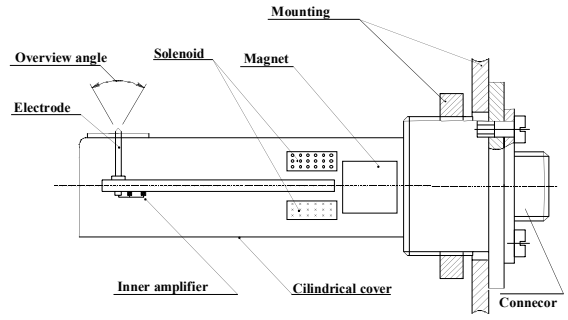

Figure 4: Electric Field Strength Sensor

The ion current density sensors used on-board Express–A #2 were two-grid Faraday probes (designated DRT). The first grid was held at spacecraft potential. The second grid was biased 40 Volts negative with respect to the spacecraft potential in order to repel incident electrons. A final disk electrode was then used to collect the remaining ion current. Each grid was 60% transparent. Both the grids and the collector were fabricated from stainless steel. The effective collection area was 1 square centimeter. The error in the calibrated current measurement was estimated to be less than 15%. This sensor is shown schematically in Figure 5.

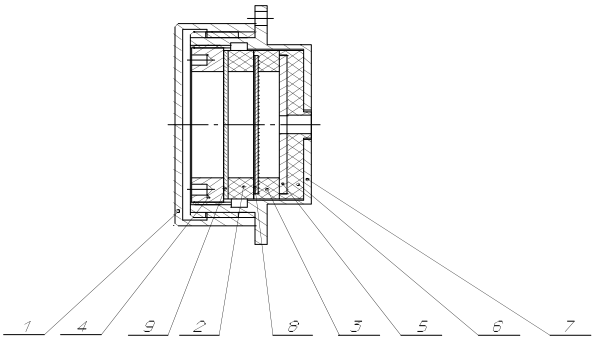

Figure 5: Ion Current Density Sensor (1- removable protective cover, 2,3,6 – Teflon insulators, 4- clasping nut, 5- collector, 7- probe body, 8 – screen grid, 9, electron repelling grid).

Two of the electric field strength sensors were located on the body of Express-A #2's thermal radiator (DEP1 & DEP2). The third electric field sensor (DEP3) was located on the communication payload. The ion current density sensors were mounted on the payload interface ring. One of the ion current density sensors (DRT2) was located underneath a multi-layer insulating thermal blanket. The location of each of the probes on-board Express-A #2 is shown in Figure 6.

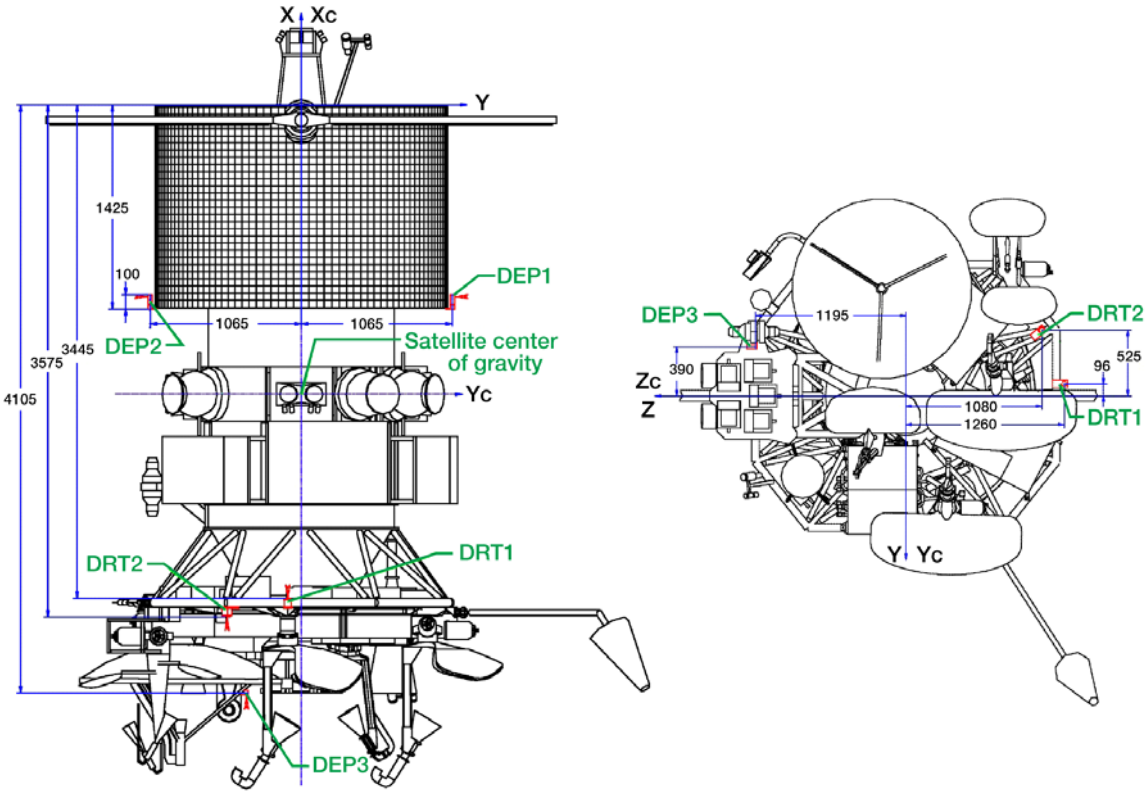

Figure 6: Sensor locations on-board Express-A #2

On-board Express-A #3 were three electric field strength sensors (designated DEP1,2,&3), two four grid retarding potential analyzers to measure ion current and energy (designated DRT3-1 & DRT3-2), two three grid retarding potential analyzers to measure ion current and energy (designated DRT1 & DRT2), and two pressure sensors (designated IMDD1&2). The electric field strength probes were of the same design and construction as those used on Express-A #2. The retarding potential analyzers were of two different configurations. The four-grid analyzer (DRT3), shown in Figure 7, was designed for use at very low plasma density. The first grid was held at spacecraft potential. The second grid was biased to – 40 Volts to repel electrons. The third grid was the ion energy selector that was biased between 0 and 350 Volts. The fourth and final grid is biased to – 20 Volts to repress secondary electron emissions. Each of the grids was fabricated from molybdenum wire and had a transparency of 0.6. Based on experimental calibration with an ion source the effective area of the probe was 0.4 square centimeters and the measurement uncertainty was less than 15%.

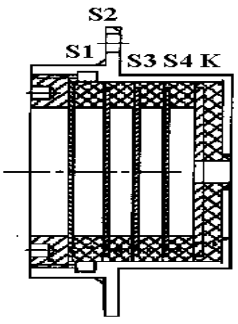

Figure 7: Four Grid Retarding Potential Analyzer (S1- screen grid, S2- cut-off grid, S3 – analyzing grid, S4 – suppressor grid, K – collector)

The three grid retarding potential analyzers (DRT) were similar in concept to the four grid sensors with the omission of the forth grid for suppression of secondary electron emission. The grids were fabricated from stainless steel and had transparencies of 0.54, 0.49, and 0.52 for the screen grid, the electron repelling grid,

and the ion selecting grid respectively. Based on experimental calibration with an ion source the effective area of the probe was 0.4 square centimeters and the measurement uncertainty was less than 15%. This probe is shown schematically in Figure 8.

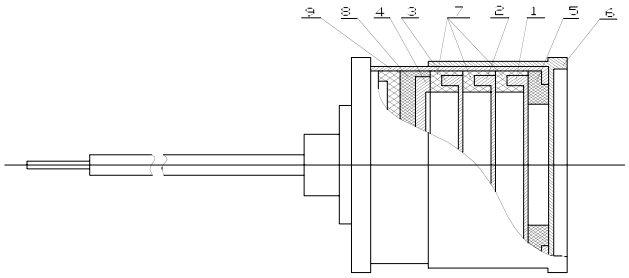

Figure 8: Three Grid Retarding Potential Analyzer (1 – screen grid, 2 – cut-off grid, 3 – analyzing grid, 4 – collector, 5 – diaphragm, 6 – removable cover, 7 - isolating ring, 8 – isolator, 9 – body)

The pressure probes (IMDD) were of an "inversion magnetron" type. This type of probe was chosen for its accuracy and vibration resistance as compared to traditional ionization gauges, which typically utilize a thin tungsten filament. This sensor is shown schematically in Figure 9.

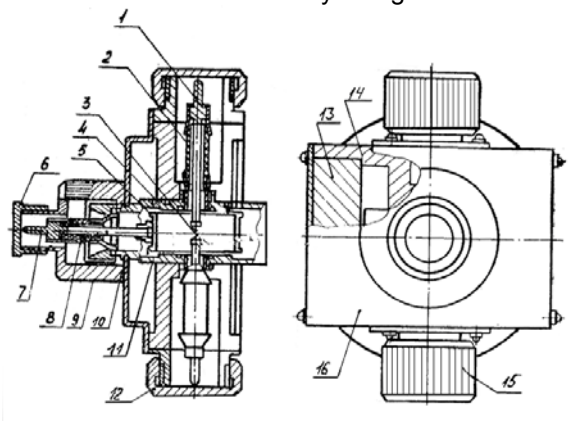

Figure 9: Pressure Sensor (1- anode inputs; 2 - ceramic isolators, 3 - anode, 4 & 11 - face covers of the anode, 5 - cathode, 6 - stub, 7 - cathode input, 8 - ceramic isolators, 9 - nut to fix the magnet, 10 - sensor body, 12 - thread-sleeves to attach high-voltage plugs, 13 - one of two magnet-bars, 14 - polar tip of the magnet, 15 - cap on the anode outputs, 16 – magnet).

The locations of these various probes are shown in Figure 10. The electric field sensors were located on the thermal radiator and payload as on Express-A #2. The two four-grid ion energy analyzers (DRT3) were located on the payload interface ring as were the DRT Faraday probes on Express-A #2. The pressure probes (IMDD) were located immediately adjacent to these probes to allow for the correlation of ion current density with pressure. The IMDD2 and the DRT3-2 sensors were located under the multi-layer insulation. The two three-grid ion energy probes were located on the solar arrays. The DRT1 probe was located on the array on the south side of the spacecraft. DTR2 was on the array on the north side of the spacecraft. The DRT sensors were oriented with their axis parallel to the axis of solar array rotation. The locations of each of the probes on-board Express-A #2 are shown in Figure 10.

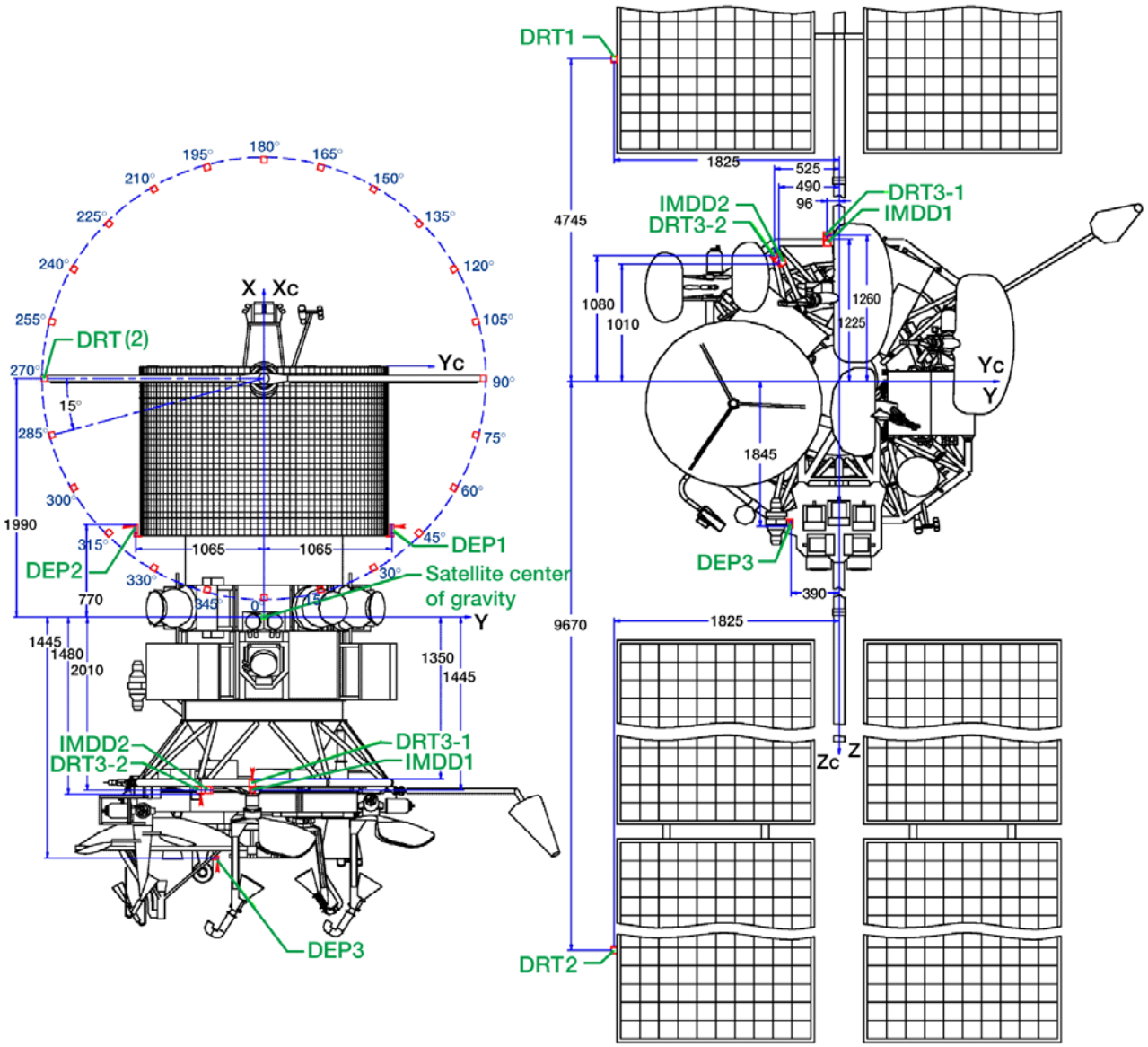

Figure 10: Sensor locations on-board Express-A #3

Results

Momentum Transfer

On-board both Express-A #2 and Express-A #3 SPT-100 propulsion systems were successfully functioned at least twice in every configuration during initial check out, were then used to perform final orbital corrections placing the spacecraft on station, and then began performing North-South and East-West station-keeping. In all cases the propulsion system executed the operational commands according to the specified logic. No anomalous behavior was observed during these operations. During initial drifting and transfer phases the effective thrust of several of the thrusters in the East-West direction were determined using orbital parameters from range data. Similarly the effective thrust of the North-South orbit control thrusters was determined from range data between successive cycles during which the thrusters were operated. These data are tabulated in Table 4.

Table 4: Effective Thrust for Thrusters on-board Express-A #2 and Express-A #3

Satellite	Date	Thruster	Cathode	Effective Thrust, mN
Express-A #2	3/17/00-3/18/00	T2	C1	80.3
Express-A #2	3/19/00-3/20/00	T2	C1	79.5

Express-A #2	4/28/00-4/30/00	RT2	C1	81.5
Express-A #2	5/8/00-5/9/00	T1	C1	81.0
Express-A #2	5/11/00-5/12/00	RT1	C1	82.5
Express-A #2	5/15/00-5/28/00	T3, RT3	C1	70.5
Express-A #2	6/1/00-6/13/00	T3, RT3	C1	73.1
Express-A #3	7/16/00-7/18/00	RT1	C1	81.4
Express-A #3	7/20/00-7/22/00	RT1	C1	83.0
Express-A #3	7/24/00	RT1	C1	83.8
Express-A #3	8/20/00-9/1/00	T3, RT3	C1	65.0
Express-A #3	9/5/00-9/15/00	T3, RT3	C1	74.0
Express-A #3	9/19/00-9/29/00	T4, RT4	C1	85.0

It is apparent from these data that the effective thrust on-orbit is less than that measured during acceptance testing. For all thrusters other than T3 and RT3 the effective thrust was within 8% of the values measured during acceptance testing. It also appeared that over time the effective thrust increased. This is consistent with a twenty-hour on-orbit "burn-in" time claimed by the thruster manufacturer.[10] Over the duration of this period the performance of the thrusters was thought to stabilize gradually, increasing to some steady-state value. For thrusters T3 and RT3 the discrepancy between the effective thrust and the acceptance test values was considerably larger. These thrusters were located on the North facing side of the satellites. As a result there was a significantly larger opportunity for momentum transfer due to plume impingement on the solar array. This effect should also be manifest for thrusters T4 and RT4 on the South side of the spacecraft. It is possible, however, for the firings between 9/19/00 and 9/29/00 the solar array was favorably aligned to minimize this effect during the firings of T4 and RT4. The angular position of the solar array during these firings was not provided. Additionally, the small change in performance due to slightly higher discharge voltage and current on-orbit was not considered.

The effect of momentum transfer due to plume impingement was also demonstrated by the disturbance torques induced on the spacecraft from thruster firings as determined from the reaction of the attitude control system. These data, which were gathered during both the final orbital positioning portion of the mission and during the station-keeping phase of operation, were used to determine the torque induced in each of the directions on the spacecraft. These data are shown in Table 5. The x-axis points towards the Earth. The y-axis points westward, and the z-axis points northward.

Table 5: Disturbance Torques Measured on-board Express-A #2 and Express-A #3

Satellite	Thruster	Cathode	SA Angle	Date	Torque, N-m x 10^3		
					X	Y	Z
Express-A #2	T2	C1	180	3/17/00	-0.897	-0.467	-0.923
Express-A #2	T2	C1	255	3/17/00	-0.922	0.132	-1.17
Express-A #2	RT2	C1	180	4/29/00	-1.07	-0.088	0.007
Express-A #2	T1	C1	180	5/8/00	1.41	-0.548	5.46
Express-A #2	T4	C1	105	4/12/00	-1.87	-3.50	-0.304
Express-A #2	T4	C1	120	4/12/00	-2.56	-2.51	-0.277
Express-A #2	RT4	C1	105	4/13/00	-1.45	-2.55	-0.016
Express-A #2	RT4	C1	120	4/13/00	-2.53	-3.61	0.198
Express-A #2	T4	C1	30	4/15/00	1.55	-0.932	0.154
Express-A #2	T4	C1	45	4/15/00	1.97	-2.70	0.010
Express-A #2	T4	C1	30	4/16/00	1.69	-0.943	0.150
Express-A #2	T4	C1	45	4/16/00	1.97	-2.77	0.019
Express-A #2	T4	C1	60	4/16/00	1.57	-3.93	0.169
Express-A #2	T4	C1	30	4/17/00	1.73	-0.967	0.134
Express-A #2	T3	C1	150	4/22/00	1.52	4.14	0.220
Express-A #2	T3	C1	165	4/22/00	0.629	2.38	0.200
Express-A #2	RT3	C1	135	5/23/00	3.56	4.20	-0.276
Express-A #2	RT3	C1	150	5/23/00	3.42	3.35	-0.388
Express-A #2	RT3	C1	105	6/11/00	2.07	6.78	-0.376
Express-A #3	RT3	C1	75	7/2/00	-1.33	5.86	-0.113
Express-A #3	T3	C1	105	7/2/00	-0.500	6.62	0.430
Express-A #3	RT4	C1	240	7/2/00	6.92	-10.2	1.05
Express-A #3	T4	C1	270	7/2/00	-0.631	-14.2	-0.285
Express-A #3	RT3	C1	45	8/7/00	-3.04	4.76	0.102

Express-A #3	RT3	C1	60	8/7/00	-2.61	5.80	-0.045
Express-A #3	RT3	C1	30	8/23/00	-2.89	3.21	0.240
Express-A #3	RT3	C1	45	8/23/00	-3.27	5.13	0.067
Express-A #3	T3	C1	30	8/24/00	-3.62	3.20	0.527
Express-A #3	T3	C1	45	8/24/00	-4.01	4.32	0.594
Express-A #3	RT4	C1	180	9/19/00	1.15	3.56	-0.284

The largest disturbance torque was encountered in the Y direction when firing thruster on the north or south side of the spacecraft. For these cases the possibility for interaction of the plume from the thruster with the solar arrays was the greatest. Induced torques on the spacecraft due to plume impact were also estimated using a two-dimensional plume code[11] and the three-dimensional Environment Work Bench[12], recently updated with a model to predict induced moments on a spacecraft during thruster operation.[13] Both specular and diffuse solar array surfaces were considered in assessing the effects of the incident ion flux from the thruster. These predictions as well as the values measured on-orbit are shown graphically in Figure 11 for torques induced around the x-axis. Generally the data seems to substantiate a specular type interaction. Past Russian experience with induced torques have suggested a more diffuse reaction with the back-side of the solar array.[14] However, the design and construction of the solar arrays used by past spacecraft may have been different than those used on Express-A #2 and Express-A #3.

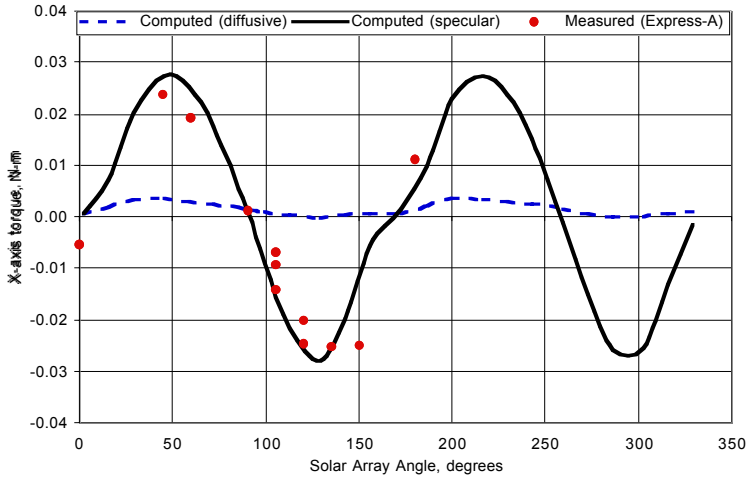

Figure 11: X-axis disturbance torque flight data predicted values based on both absorptive and reflective surfaces.

Communications

For both Express-A #2 and Express-A #3 the possibility for the plasma thrusters to interfere with communication payload was investigated. The Q-factor and interference levels on Express-A #2 were measured on 4/12/00 and 4/13/00 both before and during thruster operation. No anomalous performance was detected during thruster operation. These same measurements were made on Express-A #3 on 8/7/00 and 8/8/00 with the same result. There were also no discernable effects on the transmission and reception of command and telemetry signals during thruster operation.

Ion Current Density

Using the fixed DRT sensors on Express-A #2, the fixed DRT3 sensors on Express-A #3, and the movable DRT sensors on the arrays on-board Express-A #3 the ion current density was measured. Because eight different thrusters were fired, there were a significant number of different geometric configurations that were achieved. In some cases various portions of the spacecraft were between the thruster which was fired and the ion current density sensors. In those cases there was negligible or reduced ion current at the sensor. All these data were normalized to a distance of 1 meter from the thruster using a $1/r^2$ correction. The non-zero experimental data are shown in Figure 12 along with three curves: calculated values for a finite background pressure of 2×10^{-6} Torr, calculated values for no background, and experimental data measured at 2×10^{-6} Torr. The calculated data assumed a mass flow rate of 5.3 mg/s which may have been slightly higher than that on-orbit.

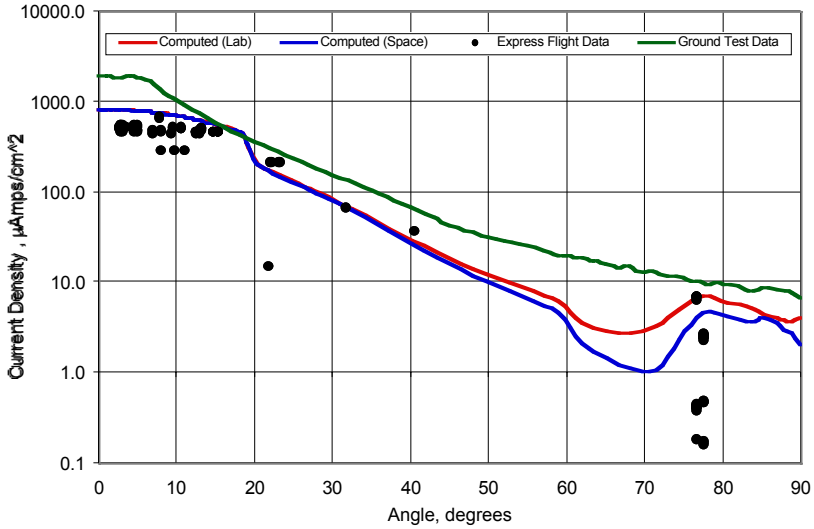

Figure 12: Ion Current Density versus Angle

For angles of thirty degrees or less the values calculated using the plume model [Ref 11] agree moderately well with the Express data regardless of the background pressure. The agreement at angles less than 10 degrees could have been improved further by varying the electron temperature chosen for the initial condition. A value of 8 electron Volts was used for these calculations. Increasing the value by one to two electron Volts would decrease the value at small angles while simultaneously depressing the calculated density at large angles. There was not a large amount of data at larger angles and there was a substantial amount of scatter among these points. At approximately 77 degrees there are a number of points. The two upper-most groups of points are taken with DRT1 on-board Express-A #2. The higher values are data measured with RT4 firing. The lower values are for T4. There is an approximately 1 degree angular difference and a 10 cm radial difference in the position of these thrusters relative to the current density sensor. Yet there was consistently a factor of three difference in the measured values. A likely explanation for this is a partial geometric obstruction between T4 and DRT1, although this could not be confirmed. This may also explain the single point with relatively low ion current at 22 degrees.

This difference in measured ion current values at 77 degrees for thruster RT4 versus T4 was also present on Express-A #3, although the overall values were an order of magnitude lower. While both the DRT1 probe on Express-A #2 and the DRT3-1 probe on Express-A #3 used to make these measurements were gridded, the impact of using these probes at an approximately 75 degree angle with respect to the incoming ions as opposed to normal orientation was not investigated.

The difference between ground test data and the calculated values is significant at all angles. These differences are attributed to the use of an un-collimated probe and collisional processes occurring in the ground test facility. These processes are thought to include both elastic scattering processes and charge exchange collisions. These effects which have been recently investigated in detail by Pollard, et al.[15] and modeled by Katz et al.[11] would tend to result in elevated values of ion current density at large angles with significant back pressure. Furthermore, the calculations conducted at the measured background pressure suggest that the actual pressure near the thruster may have been as much as two to three times higher than that reported as measured by an ion pressure gauge along the wall of the test facility. Also, the use of the un-collimated probe for the ground test would result in elevated values of ion current density with respect to the effective partially collimated gridded probes.

As a result of the differences between the flight data, the calculated values, and the ground test data significant uncertainty remains with respect to understanding the potential differences between the ion current density distribution in test facilities compared to that in space. In order to mitigate this uncertainty, additional ground test investigations would need to be undertaken to consider the effect of using probes of this type on-orbit.

Ion Energy

In addition to measuring ion current density, the gridded probes on Express-A #3 were used to measure the ion current collected as a function of the repelling voltage on the analyzer grid. An example of this raw data as measured by DRT1 is shown in Figure 13. These data can then be differentiated with respect to the applied voltage to determine the distribution of ions with respect to their energy-to-charge ratio. The flight data were differentiated using a simple forward difference and the results are also shown in Figure 13. Based on this, the most probable ion energy for singly charged ions at this location, 3.8 meters from the thruster at an angle of 8 degrees, was 250 Volts. The plume model, which also calculates ion energy, predicted a most probable value of 230 Volts at this location. Because of the relatively few number of ion current measurements in the region where there was a large change in current with voltage, this agreement can be considered quite good.

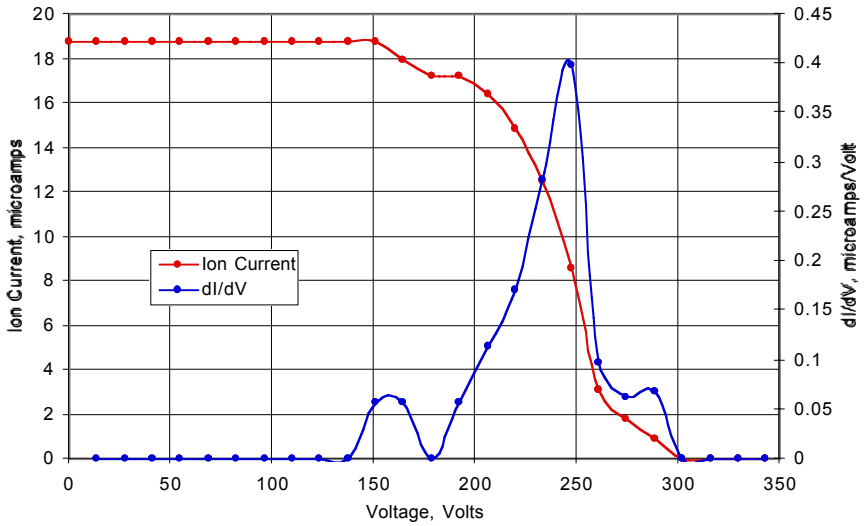

Figure 13: Ion energy sensor data and energy distribution at 3.8 meters and 8 degrees

Similar measurements taken with the DRT3 sensor, at large angles were also considered. Measurements taken at an angle of approximately 77 degrees with respect to thruster unit four measured predominately charge exchange ions as seen in Figure 14. For this location, 1.4 meters from the thruster the model predicted a most probable energy of 28 Volts. The experimental data had a peak at 27 Volts. A small indication of the primary ion beam at 240-250 Volts is also still present. This confirms the general nature of the ion energy distribution as it evolves through charge exchange as predicted by the model.

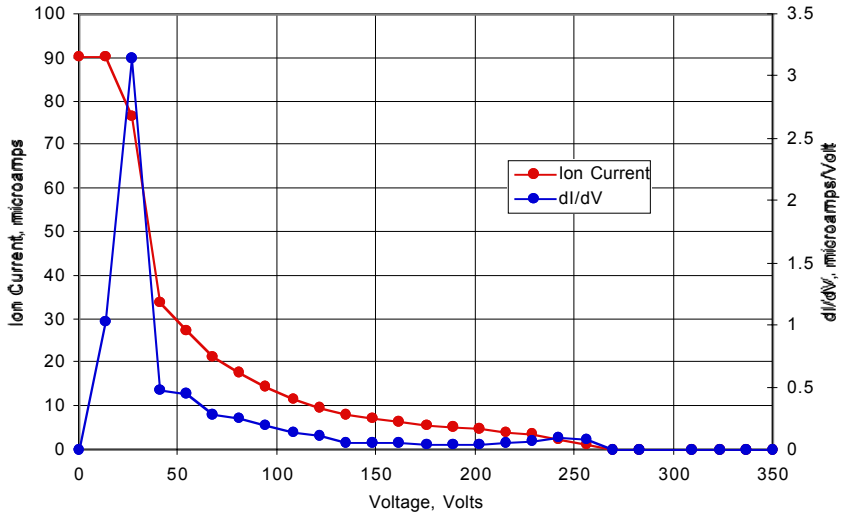

Figure 14: Ion energy sensor data and energy distribution at 1.4 meters and 77 degrees

Pressure

On Express-A #3 the two IMDD pressure sensors began operation on 6/24/00, 5 hours after separation of the spacecraft from the booster. The sensors continued to operate for approximately 8 hours until the power supply failed. This failure was attributed to the high current levels present in IMDD2, the pressure sensor located under the MLI. This sensor recorded a pressure in excess of the maximum measurable value of $7x10^{-6}$ Torr the entire time it was operated. The pressure measured by IMDD1 is shown in Figure 15 as a function of elapsed time from its initial operation. The on-board thrusters were not function until 6/29/00. The pressure data compare favorably with data from previous Russian geosynchronous communication satellites that showed pressure decreased significantly the first day on orbit and eventually stabilized at $2x10^{-8}$ Torr after 10-15 days. These previous on-orbit measurements recorded pressures as high as 10^{-5} Torr during thruster operation.

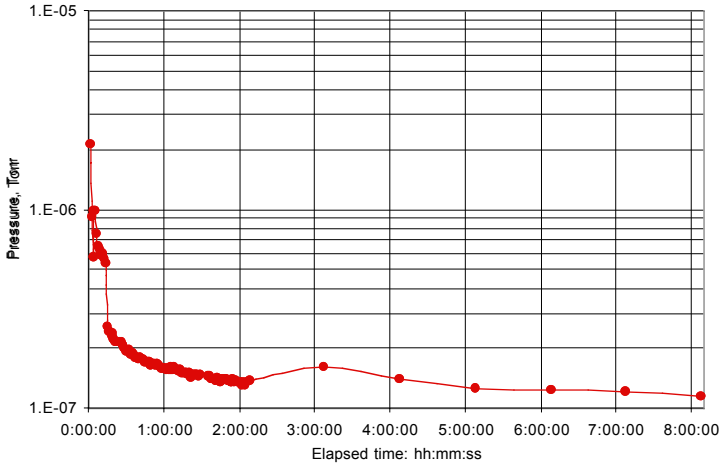

Figure 15: IMDD1 Pressure Sensor Data versus Time

Electric Field Strength

The DEP sensors on-board both Express-A #2 and Express-A #3 were used to measure electric field strength. These measurements were an attempt to address issues of differential electrostatic spacecraft charging which have been thought to have caused anomalous equipment operation on previous Russian spacecraft. Data are presented from three different 24-hour periods of electric field strength measurements on days in which thrusters were operated on-board Express-A #3. The dates were 7/8/00, 8/8/00, and 9/4/00 and the thrusters operated were RT4C1, RT3C1, and RT4C1 respectively. Figure 16a shows data corresponding to a 15 minute firing of RT4C1 from 2:51 to 3:06. The effect on the measured electric field strength for each of the sensors is small with a possible decrease in the DEP3 measurement at the time of thruster firing. Figure 16b shows data corresponding to a 60 minute firing of RT3C1 from 12:44 to 13:44. In this case there is a definite correlation to an increase in the electric field strength measured and the thruster firing. Figure 16c shows data corresponding to a 70 minute firing on RT4C1 from 21:21 to 22:31. In this case there is no discernable effect of thruster operation on the measured electric field strength, but there are significant increases in electric field strength early in the day.

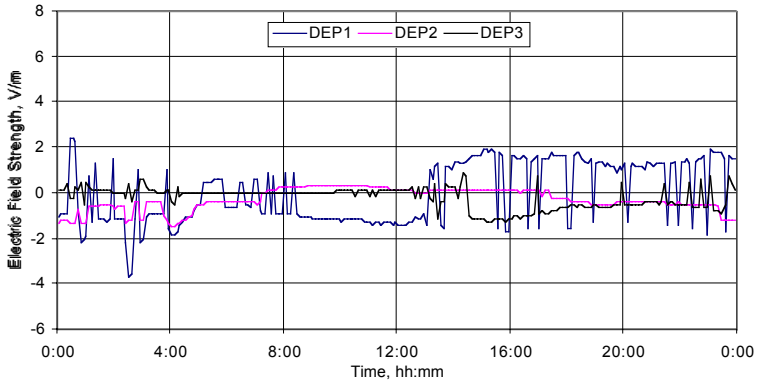

Figure 16a: Electric field strength on-board Express-A #3 7/8/00 versus Time (thruster RT4C1 was fired for 15 minutes from 2:51 to 3:06)

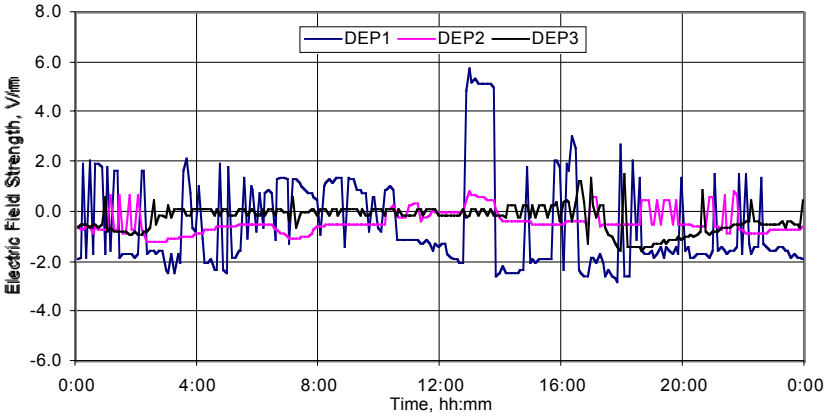

Figure 16b: Electric field strength on-board Express-A #3 8/8/00 versus Time (thruster RT3C1 was fired for 60 minutes from 12:44 to 13:44)

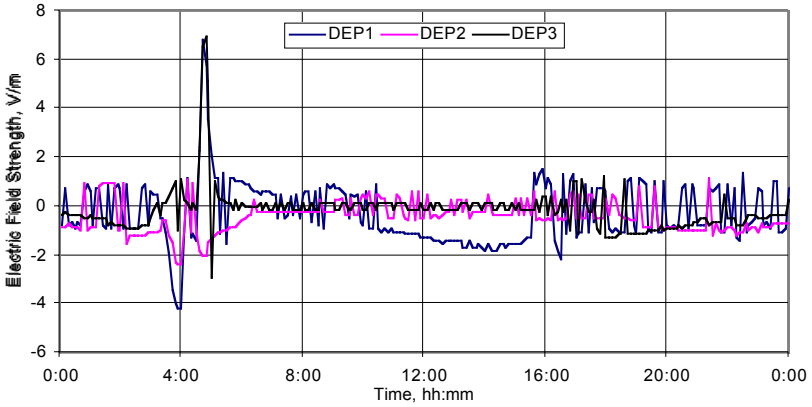

Figure 16c: Electric field strength on-board Express-A #3 9/4/00 versus Time (thruster RT4C1 was fired for 70 minutes from 21:21 to 22:31)

It is known that there are various additional environmental effects that contribute to differential electrostatic spacecraft charging such as solar intensity and geomagnetic intensity. Because these effects are not well understood by the authors it is difficult to provide any substantial interpretation of these data other than to say that in some cases there was clear evidence that thruster operation modified the electric field strength at the surface of the spacecraft. The implication of this with respect to spacecraft charging and the magnitude of this effect relative to other potential influences are unknown.

Solar Array Degradation

In order to determine if there was any effect of thruster operation on the output of the solar arrays an analysis of performance of the arrays on Express-A #3 was performed. Array performance for the first four months of operation was considered. During this period solar array performance improved instead of degrading as expected. For the following three months, the performance stabilized. After seven months the array performance began to degrade. These solar array output power is shown in Figure 17 along with an estimate of the solar flux and prediction of the solar array output based on typical degradation rates for radiation and UV damage to solar cells with their integrated cover slides.

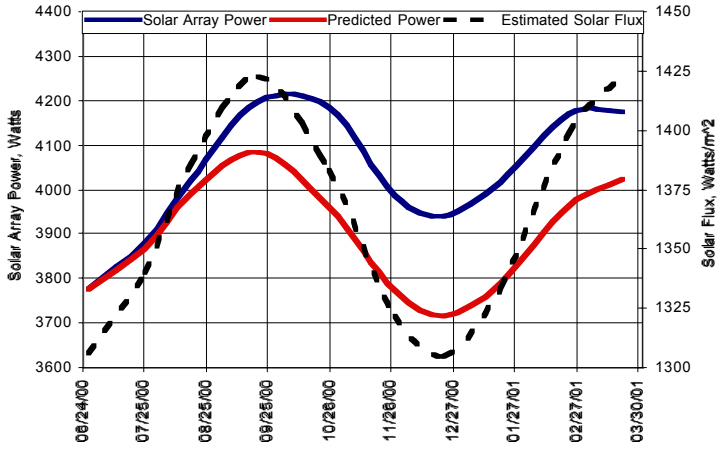

Figure 17: Solar Array Power, Predicted Solar Array Power,and Estimated solar Flux vs. Time

Figure 18 shows normalized powers versus time for the entire solar array, plus the three parts of the array that are measured separately. The normalized predicted power is also included. SA3 and SA4 are individual panels (one on each of the two wings) and the SA1 + SA2 are the total of the remaining six solar array panels (three on each wing). The data has been corrected for the estimated changes in solar flux and then normalized back to the initial performance measured two days after launch.

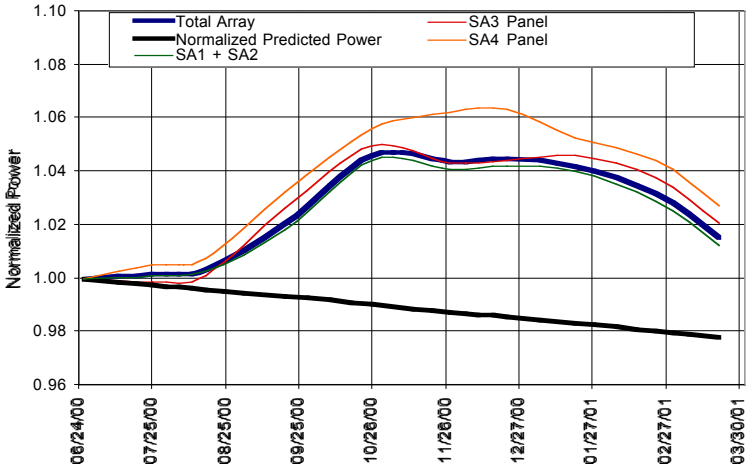

Figure 17b: Normalized Solar Array Power Curves vs. Time

One possible explanation for the reported increase in solar array output with time is based on the current being measured at a fixed voltage. Typically this voltage would be selected near the maximum power. It is possible, however, that as the array performance changed the voltage at which the maximum power was produced also changed. This would introduce an error in the comparison of power measurements over time. A second possible explanation for these data is that there was an actual performance improvement from the second to fourth month due to a slow annealing process that was fixing initial damage in the solar cell materials. If the solar cells had high initial shunt currents, this would be possible. If this was the case, then the slope over the last two months of data received would indicate a higher than predicted degradation rate,

once the initial damage was repaired. This would indicate a possibility that the thruster plume was causing significant array degradation. There is no evidence to corroborate either of these potential explanations.

Conclusions

The operation of North-South and East-West station-keeping Hall thruster propulsion systems on-board the Russian Express-A #2 and Express-A #3 geosynchronous communication satellites was documented. The configuration of these spacecraft, the configuration of the propulsion system, the effect thruster operation had on the spacecraft, and individual on-board measurements were all presented. Based on ACS system data and range data momentum transfer due to plume impingement was present reducing the effective thrust of the SPT-100 thrusters and inducing measurable disturbance torques. The effect of the plasma plume produced by thruster operation was shown to be negligible with respect to the transmission of C-band and KU-band communication signals. Ion current density measurements made on-board each of the spacecraft showed that there is a difference between space and ground test data. Ion energy measurements made on orbit agree favorably with predictions based on a plume model a plume model that accounts for charge-exchange collision events that produce both low (<50 V) and high-energy (>100 V) ions at large angles. Total pressure measurements were attempted on-board Express-A #3. Initial data were obtained prior to failure of the sensor's power supply. The measured values agreed well with past measurements. Electric field strength measurements were reported. The implication of these measurements with regard to spacecraft charging was unknown. The effect of plume impingement upon solar array output was also investigated. The possible effect of the Hall thrusters on solar array performance was also inconclusive. These data represent a sample from a large body of information contained in various reports provided to NASA GRC as part of a contracted effort.

References

1. Peterson, T., et al., "The Express/T-160E Flight Hardware Development Effort," AIAA-98-3328, July 1998.
2. Peterson, T., et al., "Update of the Express/T-160E Flight Hardware Development Effort," AIAA-99-2275, June 1999.
3. Task 25 Completion Report, NASA Contract NAS3-99151, SPI Subcontract 97-1088-02, "Acquire TM Data for Type B Sensors for Express-A No2 Satellite (Period of 12 March 2000 to and including 15 June 2000)," NPO PM-Razvitie, 2001.
4. Task 27A Completion Report, NASA Contract NAS3-99151, SPI Subcontract 97-1088-02, "Acquire TM Data for Type A and Type B Sensors for Express-A No3 Satellite (Period of 24 June 2000 to and including 30 September 2000)," NPO PM-Razvitie, 2001.
5. Task 27B Completion Report, NASA Contract NAS3-99151, SPI Subcontract 97-1088-02, "Acquire TM Data for Type A and Type B Sensors for Express-A No3 Satellite (Period of 01 October 2000 to and including 31 December 2000)," NPO PM-Razvitie, 2001.
6. Task 29 Completion Report, NASA Contract NAS3-99151, SPI Subcontract 97-1088-02, "Acquire Express-A #2 SPT-100 Based Propulsion Subsystem and other Subsystem Flight Operation TM-Data for a Period of 12 March 2000 to and including 15 June 2000," NPO PM-Razvitie, 2000.
7. Task 30 Completion Report, NASA Contract NAS3-99151, SPI Subcontract 97-1088-02, "Acquire Express-A #3 SPT-100 Based Propulsion Subsystem and other Subsystem Flight Operation TM-Data for a Period of 24 June 2000 to and including 30 September 2000," NPO PM-Razvitie, 2001.
8. Task 31 Completion Report, NASA Contract NAS3-99151, SPI Subcontract 97-1088-02, "Acquire Express-A #3 SPT-100 Based Propulsion Subsystem and other Subsystem Flight Operation TM-Data for a Period of 01 October 2000 to and including 31 December 2000," NPO PM-Razvitie, 2001.
9. Task 32 Completion Report, NASA Contract NAS3-99151, SPI Subcontract 97-1088-02, "Acquire Express-A #3 SPT-100 Based Propulsion Subsystem and other Subsystem Flight Operation TM-Data for a Period of 01 January 2001 to and including 31 March 2001," NPO PM-Razvitie, 2001.
10. Personal communication Victor Petrusevich, NPO-PM, August, 2001.
11. Katz, I. et al., "A Hall Effect Thruster Plume Model Including Large-Angle Elastic Scattering," AIAA-01-3355, July 2001.
12. Gardner, B.M., G. Jongeward, B. Kuharski, K. Wilcox, T. Rankin, J. Roche, "The Environmental Workbench: A Design Tool for the International Space Station," AIAA Report 95-0599, Washington, D. C. 1995.
13. Mikellides, I.G., *et al.,* "A Hall-Effect Thruster Plume and Spacecraft Interactions Modeling Package," IEPC Paper 2001-251, Oct. 2001.
14. Task 14 Completion Report, NASA Contract NAS3-99151, SPI Subcontract 97-1088-02, "Analyze Data on the Main Types of Operating SPT Affects on Satellite Primary Structure and On-Board Systems," NPO PM-Razvitie, 1999.
15. Pollard, J., "Ion Flux, Energy, and Charge-State Measurements for the BPT-4000 Hall Thruster, "AIAA-0103351, July 2001.